Conformational Relaxation of Polyelectrolytes at a Solid–Liquid Interface

Emile Pefferkorn, Anne Christine Jean-Chronberg, and Raphaël Varoqui*

Institut Charles Sadron (CRM-EAHP) CNRS-ULP, 6, rue Boussingault, 67083 Strasbourg Cedex, France. *Received June 8, 1989; Revised Manuscript Received September 26, 1989*

ABSTRACT: The adsorption of hydrolyzed polyacrylamide onto a spherical nonporous adsorbent with $(SiO)_2AlOH$ surface sites was investigated as a function of the pH in aqueous media. The ζ potential and net charge of the adsorbent were determined as a function of pH by electrophoresis and potentiometric titration. The point of zero charge (pzc) of the amphoteric group $(SiO)_2AlOH$ is at 4.6. The isotherms obtained from batch experiments display a nonclassical shape which is related to a slow reorganization of the interface with time. Adsorption was then performed by monitoring precisely the supply of polymer to the interface as a function of time. It is shown that the final amount adsorbed depends on the rate of polymer supply to the interface, a feature which is also explained in terms of segmental "stiffness" at the interface. A systematic study of the kinetics of adsorption at various pH was then carried out. Below the pzc point, the surface has a net positive charge, and owing to long-range attractive electrostatic forces, adsorption proceeds at a fast rate. On the contrary, for pH values far above the pzc, the rate of adsorption is slowed down by the repulsive electrostatic forces. Near the pzc, the electrochemical behavior of the surface is influenced by the field energy of the ionized groups in the polymer diffuse layer. This gives rise to a remarkable cooperative effect on the kinetics, the adsorption amount versus time displaying a typical sigmoidal shape. The cooperative effect is explained in the light of simple electrostatic considerations assuming a slow segmental mobility at the interface.

Introduction

We consider an adsorbent with surface sites interacting specifically with the polymer units. When a polymer arrives in the vicinity of the surface, some of its segments establish energetically favorable interactions with the surface sites. This gives rise to a change of the polymer conformation. The time scale in which conformational rearrangements take place depends on the segmental binding energy. Recently, thickness relaxations of poly(ethylene oxide), which adsorbs on glass through hydrogen bonds, were described.[1,2] Relaxation is expected to be slow for large segmental adsorption energies. This should be the case when polyelectrolytes are adsorbed on oppositely charge surfaces through a salt linkage between opposite charges.[3] One expects then the structure of the surface layer, as well as the final adsorption amount, to depend on the way the surface layer was built. To be more precise, let us suppose, first, a batch experiment in which the bare surface is brought at time zero into contact with a large amount of polymer. Intuitively, if the mobility of segments, owing to a high binding energy, is very small, then the surface is covered in its final state by polymers not far from their solution conformation near the surface. On the other hand, if the solution concentration is increased stepwise by addition of small increments of polymers at time intervals Δt large enough to allow the surface layer to relax during Δt to a new conformation, then the amount of adsorption as well as the final conformation is expected to be much different, even though the polymer concentration in the bulk is the same at asymptotically large times. In the present paper, we describe such effects for a negatively charged polyacrylamide adsorbed on a positively charged surface.

We shall first report on results obtained by batch adsorption and compare them with data obtained by a technique in which the bulk concentration was monitored precisely as a function of time during the adsorption process. We shall also focus on a remarkable kinetic cooperative effect which finds also its origin in the slow polymer reconformation in presence of amphoteric surface sites.

Table I
Characteristics of Polymer Sample

polymer sample	M_w	M_w/M_n	τ, %
F2			15.5
F4	8.5×10^5	1.4	24.3
PAAC	9.6×10^5		100

Experimental Section

Polymer. Radioactive polyacrylamide with different degrees of hydrolysis, τ, was prepared as described elsewhere.[4,5] The

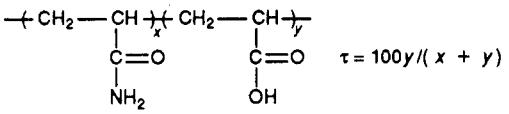

polyacrylamide contained a minute amount ($\simeq$0.1%) of a radioactive comonomer–$CH_2CH(^3HCH_2OH)$– with a specific radioactivity of 0.05 mCi/g.

Since PAM does not undergo thermal degradation during moderate hydrolysis, the F2 and F4 samples which are originating before hydrolysis from the same parent sample, $M_w = 8.3 \times 10^5$, $M_w/M_n = 1.3$, should have the same M_w and M_w/M_n ratio. The degree of dissociation α of carboxylic acid groups $CH_2CH(COOH)$ as a function of pH verifies the following relationships:[6]

$$\tau = 15.5\%; \quad \mathrm{pH} - \log \alpha/(1-\alpha) = 4.37 + 1.06\alpha + 0.193\alpha^2$$

$$\tau = 24.3\%; \quad \mathrm{pH} - \log \alpha/(1-\alpha) = 4.60 + 1.48\alpha - 0.100\alpha^2$$

Adsorbent. The adsorption measurements were performed on nonporous spherical glass beads[4,7] (code number AS(17) and AS(26)), with the following surface structure:

The $(SiO)_2AlOH$ and SiOH surface sites are distributed statistically over the surface. All details concerning the preparation and SEM picture of the adsorbent are given in refs 4 and 8, respectively.

0024-9297/90/2223-1735$02.50/0 © 1990 American Chemical Society

Table II
Characteristics of Aluminosilica Beads

sample code	average diameter, μm	specific surface area, m^2/g	surface composition[a] [Al]/[Si], %
AS(17)	34	7.8×10^{-2}	17
AS(26)	34	7.8×10^{-2}	26

[a] [Si] is the density of SiOH groups. We have chosen, according to Sears,[9] a value of 8 SiOH/100 Å^2 before chemical treatment. A misprint appeared in ref 7 where 8 SiOH/Å^2 is quoted instead of the correct 8 SiOH/100 Å^2.

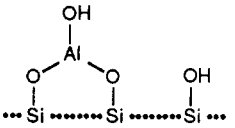

It was shown that polyacrylamide does not adsorb on nonmodified silica with 100% silanol (SiOH) surface sites. However, it interacts strongly in the presence of $(SiO)_2AlOH$ sites.[5,7] Since aluminum hydroxyde is amphoteric, we have, at a given pH, acid and base surface reactions and therefore charged and noncharged surfaces sites interating specifically with the polymer units:

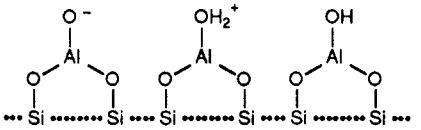

The number densities of AlOH, AlO^-, and $AlOH_2^+$ species and the ζ potential were determined in a pH range of 3–6 by potentiometric titration and electrophoresis.[5] The net charge $\sigma = eF([AlOH_2^+] - [AlO^-])$ per unit Al and the ζ potential are reported in Figure 1 as a function of pH. The net charge becomes positive at pH <4.6 and negative at pH >4.6. It should be noted that σ values measured by titration are generally found to be larger than the σ calculated from ζ potential, using the Gouy–Chapman equation and taking for the surface potential the ζ potential. As seen in Figure 1, this trend is not observed on the high-pH side. In the calculation of σ, the ionization of silica was neglected. The ionization of SiOH is indeed compared to the ionization of AlOH, negligibly small as long as pH <5. For pH >5, it might be possible however that the ionization of silanols[5] contributes somewhat to σ. This parameter is then underestimated at pH >4.6. Since in our explanation and interpretation we do not need the exact values of σ—only the pzc location is needed with precision—this point need not trouble us.

Adsorption Kinetics

Batch Adsorption. To a polyethylene vial containing 1 g of beads dispersed in water and adjusted to a given pH was added a solution of radioactive polymers at the same pH. The vial was tightly closed and its content (18 mL) mixed by gentle inversion during a determined time. The beads were allowed to settle, and the supernatant was analyzed for radioactivity content. The specific adsorption C_s (mg/m^2) was determined by

$$C_s = VS^{-1}(C_{b,o} - C_b) \quad (1)$$

V is the volume of the solution, S the total surface, and $C_{b,o} - C_b$ the difference in concentration of the supernatant before and after adsorption. $C_{b,o}$ and C_b were determined from the radioactivity of the solution.

Adsorption Kinetics. We used a technique already described in the determination of the exchange rate of adsorbed and nonadsorbed polymers.[4,10] A radioactive polymer solution of concentration C_0 is introduced at a constant flow rate J_v at orifice a of the cell—see Figure 2—of 50-mL volume containing the dispersed adsorbent. The eluent is collected at orifice b and its polymer content analyzed by radioactive counting.

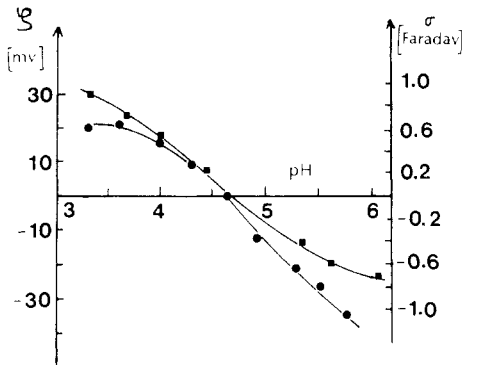

Figure 1. ζ potential (●) (left ordinate) and net charge σ (■) (right ordinate) of aluminosilica beads as a function of pH.

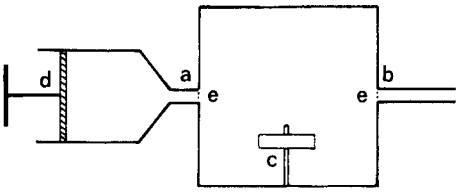

Figure 2. Diagrammatic representation of the cell used in controlled adsorption kinetics: (a, b) inlet and outlet for polymer solution, (c) magnetic bar, (d) automatically driven syringe, (e) filter.

The adsorption which proceeded under controlled agitation could be determined with precision as a function of time from the equation expressing the conservation of radioactivity:

$$J_v A_o t = VA_b(t) + SA_s(t) + J_v \int_0^t A_b(t)\,dt \quad (2)$$

A is a specific radioactivity, and subscripts o, b, and s refer respectively to the solution injected at orifice a (cpm/mL), to the effluent at b (cpm/mL), and to the surface of the beads (cpm/m^2). Since agitation is maintained throughout, A_b is also the specific radioactivity of the solution in the cell. The effluent was collected by fractions of 0.5 mL after each time interval Δt of 1 min. The differences $A_{b,i+1} - A_{b,i}$ in specific radioactivity of samples collected at times $i\Delta t$ and $(i + 1)\Delta t$ (i = 1, 2, ..., n) were small so that, to good precision, the following approximation could be used:

$$\int_0^t A_b(t)\,dt \simeq \Delta t \sum_{i=1}^{n} A_{b,i} \quad (3)$$

Specific radioactivity and polymer concentration are proportional:

$$C = A/A_{sp} \quad (4)$$

A_{sp} being the partial specific radioactivity (cpm/g).

The assumption that A_b represents the concentration throughout the cell assumes perfect mixing. This has been tested by recording the activity of the effluent in the absence of glass beads and in the presence of nonadsorbing glass beads. The latter were nonporous spherical glass beads of the same origin as AS(17) and AS(26) but with 100% SiOH surface groups and no AlOH present. In the absence of glass beads, $A_s(t) = 0$, and from eq 2, the following relation is derived:

$$A_b = A_o[1 - \exp(-J_v t/V)] \quad (5)$$

As seen in Figure 3, eq 5 is very well obeyed, and the assumption that A_b is the specific radioactivity in the

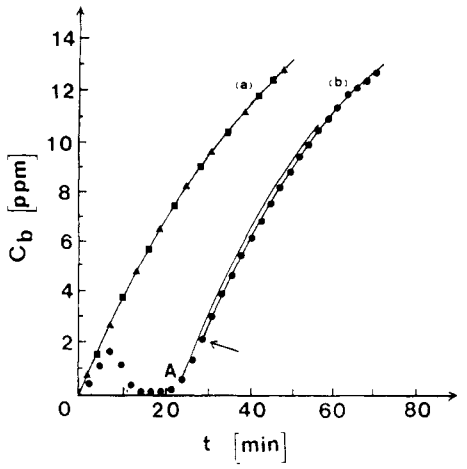

Figure 3. Variation of the effluent as a function of time. Curve a: (—) calculated from eq 5; (■) activity recorded in the absence of glass beads; (▲) activity recorded in the presence of nonadsorbing glass beads. Curve (b): (●) Activity recorded in the presence of adsorption of F2 on sorbent AS(16) at pH 5.05; (—) calculated according to eq 6; the arrow indicates completion of adsorption.

cell (perfect mixing) is justified. No special attempt was made to characterize the field flow of solution in the vicinity of the glass beads. It could nevertheless be ascertained that the effect of stagnant layers around the glass beads is negligible.[4,7] We note first that eq 5 could not be obeyed assuming a large unstirred Nernst–Planck layer around nonadsorbing glass beads. Furthermore, in our previous work,[7] an estimate of the diffusion layer thickness was obtained from the solution of Fick's law. The calculated diffusion layer thickness was indeed found to be very small (of the order of polymer dimensions, cf. the discussion and particularly eqs 1–8 and paragraph 2.2 in ref 7). The kinetic data are therefore not blurred by the effect of mass transfer by diffusion of polymers to the surface, a process which depends heavily on hydrodynamic conditions and which presents no interest on its own.

From eqs 2 and 3, the amount $C_s(t)$ of polymer adsorbed per unit surface area can be determined at any time. The completion of adsorption corresponding to a surface concentration denoted $C_{s,f}$ at time t_f can in principle be determined from the behavior of $C_s(t)$ at large time. In practice, we determined $C_{s,f}$ from the variation $C_b(t)$ of the polymer concentration in the liquid phase: eq 2 was solved with respect to $A_b(t)$ with $dA_s/dt = 0$. Using eq 5, we obtain

$$C_b(t) = C_o + (C_{b,f} - C_o) \exp[(-J_v/V)(t - t_f)] \quad (6)$$

$$t = n_i\Delta t; \quad t_f = n_f\Delta t \quad (7)$$

$C_{b,f}$ is the concentration of the effluent at time t_f, and eq 6 shows that $C_b(t)$ reaches exponentially the value C_o for $t \gg t_f$. $C_{b,f}$ was determined graphically by fitting at large time the experimental curve $C_b(t)$ with the curve predicted by eq 6. Once $C_{b,f}$ is determined, $C_{s,f}$ is obtained from eqs 2–4. The fitting routine procedure is illustrated in Figure 3. An experimental point A was arbitrarily selected. Suppose that A has coordinates $C_{b,f}$ and t_f, which means at A the adsorption is just complete (further adsorption cannot be detected within experimental precision and reasonable time interval). Equation 6 should then fit the part of the curve $C_b(t)$ on the right of point A. If the fitting test is negative (the curve predicted by eq 6 is then above the experimental curve, cf. Figure 3), the next experimental point on the right of A is considered, and the process is repeated until superposition of experimental points and eq 6 are achieved. In general, the two curves generated by eq 6 at t_f and $t_f - \Delta t$ are distinguishable, and thus the error $\Delta C_{b,f}$ on $C_{b,f}$ is proportional to Δt:

$$\Delta C_{b,f} \simeq (C_{b,f} - C_o)\frac{J_v}{V}\Delta t \quad (8)$$

$$S\Delta C_{s,f} \simeq C_{b,f}J_v\Delta t - \frac{(J_v\Delta t)^2}{V}(C_{b,f} - C_o) \quad (9)$$

From eqs 8 and 9, is can be shown that the end point of adsorption is determined with a relative precision better than 1%.

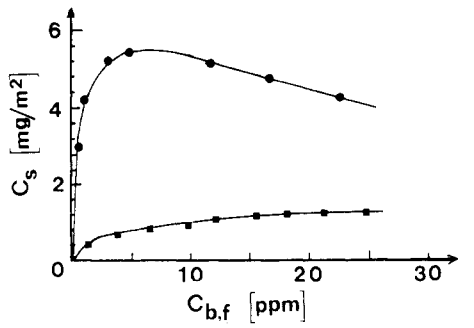

Figure 4. Batch experiment. Adsorbed amount of polymer fraction F2 on sorbent AS(26) as a function of bulk concentration after 12 h: (●) pH 4.7; (■) pH 3.3.

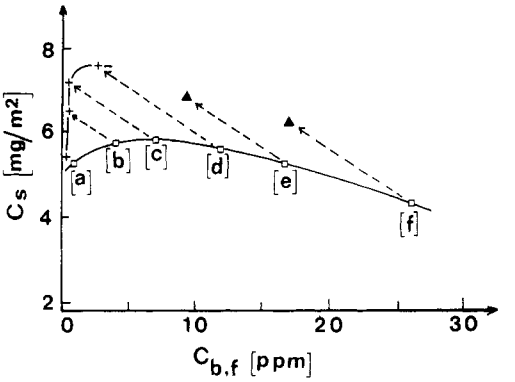

Figure 5. Batch experiment. Adsorbed amount of polymer F2 on sorbent AS(17) as a function of bulk concentration at pH 4.2: (□) after 12 hrs; (+) after 60 h; (▲) after 80 h. Initial concentration (ppm): (a) 18.6; (b) 23.5; (c) 26.9; (d) 31.5; (e) 34.8; (f) 43.0.

Results and Discussion

Batch Adsorption. Batch adsorption was carried out at 25 °C by adding a given amount of polymer to a dispersion of adsorbent AS(17) and AS(26) maintained at a constant pH.

Adsorption isotherms of polymer F2 (τ = 15.5%) at different pHs are displayed in Figures 4 and 5. The adsorption amount C_s (mg/m²) was recorded after 12 h of contact of sorbent and solution. The final polymer concentration $C_{b,f}$ of the supernatant solution is reported on the abscissa. At pH 4.7 and 4.2, the isotherms are characterized by a sharp initial rise followed by a maxima, whereas at pH 3.3 the adsorption gradually reaches a saturation plateau. The shape of the isotherms at pH 4.2 and 4.7 suggests a nonthermodynamic equilibrium state which is corroborated by the additional set of data reported in Figure 5: after the first 12 h, the suspension at pH 4.2 was left under agitatioon for 80 h and again analyzed. One observed then for C_s and $C_{b,f}$ a shift toward larger

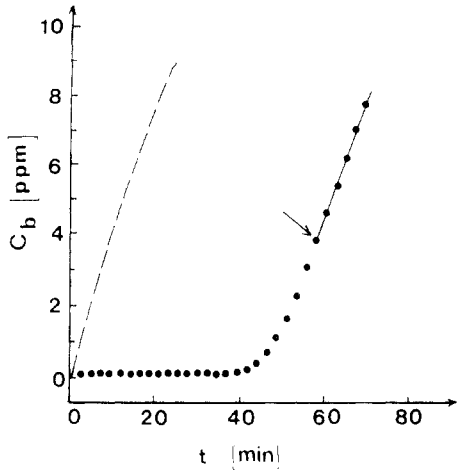

Figure 6. Kinetics of adsorption of polymer F4 on sorbent AS(26) at pH 4.39. Polymer concentration in the cell: (●) experimental point; (- - -) in the absence of adsorbent; (—) calculated according to eq 6. The arrow indicates completion of adsorption.

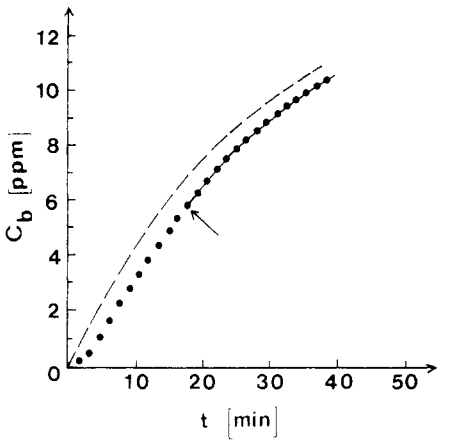

Figure 7. Kinetics of adsorption of polymer F2 on sorbent AS(26) at pH 6.0. Polymer concentration in the cell: (●) experimental point; (- - -) in the absence of adsorbent; (—) calculated according to eq 6. The arrow indicates completion of adsorption.

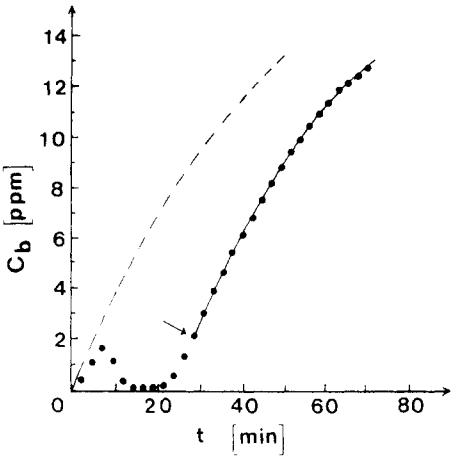

Figure 8. Kinetics of adsorption of polymer F2 on sorbent AS(26) at pH 5.05. Polymer concentration in the cell: (●) experimental point; (- - -) in the absence of adsorbent; (—) calculated according to eq 6. The arrow indicates completion of adsorption.

C_s and smaller $C_{b,f}$ values. This indicates a very slow reorganization of the interface. The underlying mechanism should be the following: in a batch experiment, the concentration of polymer in the vicinity of the interface is large, and thus a large number of polymes are adsorbed at once in a conformation near to their solution conformation. For additional polymer to adsorb, some of the attached segments of the previously adsorbed molecules must desorb, resulting in larger loops and increased film thickness. Since attachment proceeds through ion pairing (a positive–negative salt linkage), the segmental mobility and conformational rearrangement are exceedingly slow owing to the huge energy of ion pairs. A state of thermodynamic equilibrium is therefore not reached in a batch experiment. At pH 3.3, the polymer is almost uncharged, and this effect is not observed as adsorption proceeds then mainly through hydrogen bonding of amide groups on residual alumina hydroxyls.

Large time effects were seldom observed for noncharged polymers. By ellipsometry, the adsorbed film thickness of polystyrene was found to reach its equilibrium value within a few minutes.[11] The fraction of adsorbed polystyrene segments was also found to decrease with increasing bulk concentration without significant time lag effects.[12] Batch isotherms with maxima were reported by Joppien[13] for poly(oxyethylene) adsorption on the silica–water interface. Foissy et al. also reported negative slopes for the isotherms of poly(acrylic acid) adsorbed in the presence of Ca^{2+} ions onto titanium dioxide.[14]

Kinetically Controlled Adsorption. The adsorption was performed as described previously (cf. Figure 2), with the supply of polymer to the cell monitored as a function of time. The concentration of the polymer in the nonadsorbed state (measured in the effluent) is represented as a function of time for adsorption on sorbent AS(26) for the systems: fraction F4 at pH 4.39 (Figure 6), fraction F2 at pH 6.00 (Figure 7), and pH 5.05 (Figure 8); $J_v C_o/S$ was 0.128 mg/min per m^2. In Figure 9 is also shown the polymer concentration for the nonhydrolyzed PAM at pH 5.2.

From Figure 6, we note the concentration remains in the limit of experimental detection (always zero up to 40 min). The completion of adsorption indicated by the arrow occurs at 58 min. Below the pzc of the adsorbent, the very large rate of adsorption is actually controlled by the rate of polymer supply. The situation is quite different at pH 6.0. The concentration does not depart much from the concentration recorded in the absence of sorbent, and the adsorption rate is comparatively small. The same behavior holds for nonhydrolyzed PAM as seen in Figure 9. The two different situation are readily explained: at pH 4.39, a fraction of the polymer carboxylic groups is dissociated, and according to the electrophoretic measurements, the surface has a net positive charge (cf. Figure 1); the polymer is therefore accelerated toward the surface by long-range electrostatic forces. On the other hand, at pH 5.6, the surface is negatively charged, and the rate of adsorption is slowed down by the long-range repulsive electrostatic forces. In the latter case, only hydrogen bonding between the AlOH neutral form and the amide group permits polymer adsorption, negative ions being repelled and pushed away from the surface.

Focusing now on Figure 8, which corresponds to a situation where the pH is slightly above the pzc, we note the occurrence of a maximum in the variation of C_b. Adsorption proceeds first slowly (up to the maximum, the bulk concentration is not much different from the reference concentration recorded in absence of sorbent). After the maximum value is reached, the concentration decreases to zero, and within a period of 14–21 min, the rate of adsorption is very large since no more polyelectrolyte can be detected in the solution. In Figure 10, we

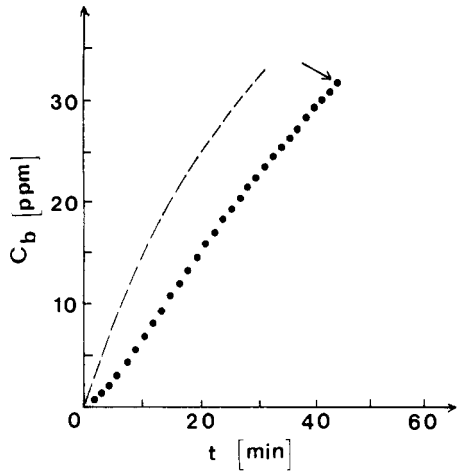

Figure 9. Kinetics of adsorption of PAM (M_w = 8.3 × 10^5). Polymer concentration in the cell: (●) experimental point; (- - -) in the absence of adsorbent; (—) calculated according to eq 6. The arrow indicates completion of adsorption.

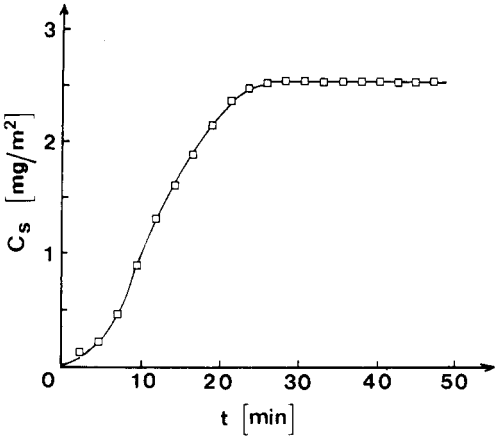

Figure 10. Adsorption amount as a function of time for polymer F2 on sorbent AS(26) at pH 5.05.

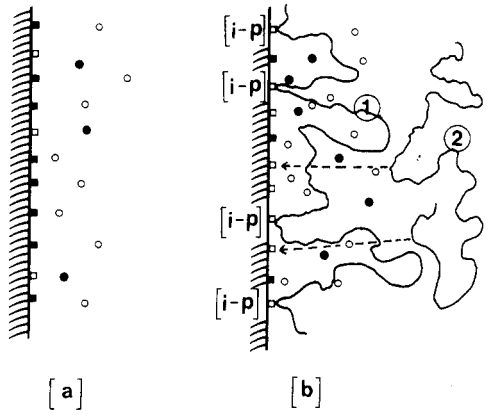

Figure 11. Schematic representation of the surface charges at pH 5.05: (a) bare surface; (b) surface in presence of adsorbed polymer. (■) AlO^- and (□) $AlOH_2^+$ charges; (○) counterion common to COO^- and AlO^- charges; (●) counterion to $AlOH_2^+$ charge; [i-p] $COO^-\cdots AlOH_2^+$ ion pairing.

have reported the adsorption amount C_s, calculated by eq 2 as a function of time. The sigmoidal shape is typical of a cooperative effect: the first adsorbed polymers speed up the adsorption of polymers introduced into the cell at a later time. With the schematic representations of the bare surface in Figure 11a and the surface containing adsorbed polyelectrolytes in Figure 11b, we suggest the following explanation: at a pH above pzc, the bare surface carries only a few positive charges (about 10% of AlOH is in the protonated $AlOH_2^+$ form at pH 4.8). The first adsorbed macromolecules have only a few negative charges in contact with the positive spots on the surface, and therefore they necessarily develop large charged loops. Since, owing to the thermal forces, the small mobile ions are pushed far away from the surface, the charged segments in the loop layer give rise to a negative space charge in the vicinity of the surface. The surface potential is therefore incremented by a negative quantity $\psi_{s,p}$. If $\psi_{s,p}$ is of the order or larger then $\psi_{s,o}$, $\psi_{s,o}$ being the surface potential in absence of polymers, then the equilibrium

$$AlO^- + 2\,H^+ \rightleftharpoons AlOH_2^+$$

is strongly shifted toward the right. As indicated in Figure 11b, the surface becomes then more positive, and the rate of adsorption of free polymers in the vicinity of the interface increases in the presence of the substantially larger amount of induced $AlOH_2^+$ charges. We reach then a situation corresponding to pH < pcz, which is characterized by a fast adsorption rate (Figure 6). Calculations are developed in the Appendix by using a simple model in which the diffuse layer is replaced by a layer of uniform charge density. This model is too crude for any quantitative estimates, but it nevertheless shows that the cooperative effect can be explained in the light of simple electrostatic considerations.

To some extent, the adsorption of polyelectrolyte on oppositely charged surfaces displays, despite the different topology, some analogy with the "adsorption" of a polycation on a polyanion. Upon investigation of the properties of a polyanion–polycation diblock, the linear diblock of poly(styrenesulfonate) and poly(2-vinylpyridine), we have shown that the basicity of pyridine is strongly enhanced in aqueous media in the presence of the negatively charged block.[15] We believe the phenomenon occurring here to have basically the same electrostatic origin. To enforce our explanation based on induced positive charges, we decided to supplement an additional experiment in which the adsorption of polymer and the amount of adsorbed counterions were measured simultaneously by using ^3H and ^{125}I radiotracers. To this end, the suspension at pH 5.0 contained at time zero a mixture of Cl^- and $^{125}I^-$ counterions, with a stoichiometry responding to

$$[Cl^-] + [I^-] \simeq mX[AlOH_2^+]$$

Quantities in brackets are ionic concentrations expressed in equiv/mL of solution, m is the concentration of sorbent (g/mL of solution), and X is the number of Al per gram of sorbent. A polyelectrolyte solution was also equilibrated with NaCl and $Na^{125}I$ at the same concentrations as before. The adsorption was then performed in the manner described previously. The radioactivity of the effluent is represented as a function of time in Figure 12. On the left ordinate is reported the radioactivity ^3H of the polymer in the effluent. On the right ordinate, we have the specific radioactivity of the effluent in ^{125}I (γ emitter). The activity of iodide decreases sharply up to the maximum of ^3H, which signifies that iodide ions are driven to the surface to act as counterions for "new" $AlOH_2^+$ sites appearing in presence of adsorbed polymers, confirming therefore the proposed mechanism.

The cooperative effect has always been found at a pH slightly above the pzc for HPAM of different τ value. An example for poly(acrylic acid) (τ = 100%) is shown in Figure 13 at pH 4.80.

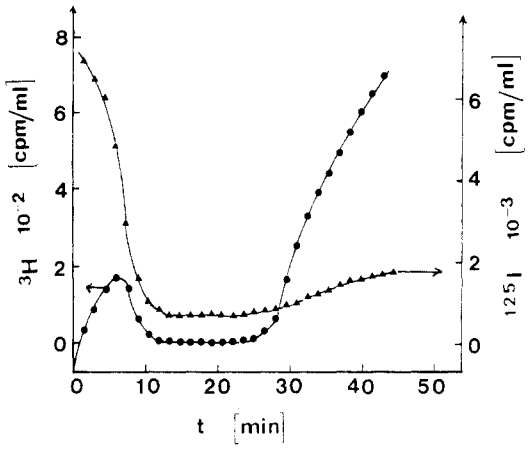

Figure 12. Variation of the activity of ^3H (●) and ^{125}I (▲) in the effluent as a function of time for polymer F2 adsorbing on AS(26) at pH 5.05.

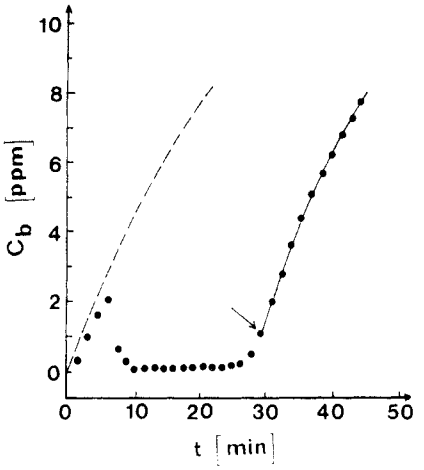

Figure 13. Kinetics of adsorption of PAAC (100% hydrolyzed) at pH 4.8. Polymer concentration in the cell: (●) experimental point; (- - -) in the absence of adsorbent; (—) calculated according to eq 6. The arrow indicates completion of adsorption.

It is important to emphasize that in trying to interpret in the light of the previous discussion the cooperative effect we are brought back to assume a slow reconformation of polyelectrolytes in the adsorbed state. Indeed, if the charged diffuse layer induces a substantial amount of positive surface charges, one could as well expect the loops of adsorbed polymer (polymer 1 in Figure 11b) to collapse on the surface. Our proposed mechanism becomes plausible only when the very "stiff" contacts [i–p] prevent easy reconformation. In the following, we shall present more evidence on the conformational relaxation in the adsorption of charged polymers.

Adsorption at Various Polymer Supply Rates. All results thus far reported were obtained at a constant value of J_vC_o/S of 0.128 mg/min per m^2. In Figure 14 is reported the final adsorption amount $C_{s,f}$ for polymer F4 at pH 4.39 as a function of the rate of polymer supply per unit surface area. $C_{s,f}$ was determined as specified in the Experimental Section, by fitting at large times the $C_b(t)$ curve with the curve predicted by eq 6. Clearly, the final adsorption amount is seen to depend on the rate of polymer supply. At small injection rates, time is allowed for the adsorbed polymer to spread on the surface and to reach a flat conformation; the average number of surface contacts per polymer is then large in the final adsorption state, and slow adsorption amounts are therefore expected. As observed, the adsorption increases with J_vC_o/S, and

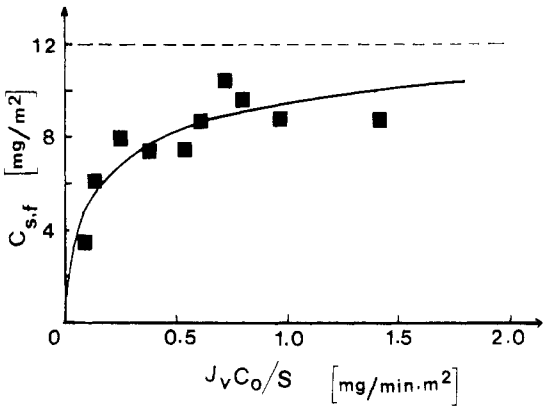

Figure 14. Adsorbed amount as a function of the rate of polymer supply.

ultimately, at very large injection rates, we are in the conditions of the batch experiments described previously.

Since conformational rearrangement is a very slow process compared to the time interval after which $C_{s,f}$ is recorded, none of the data reported in Figure 14 characterizes a situation of thermodynamic equilibrium. Experiments suggesting irreversible adsorption of polyelectrolytes were also reported by Klein and Luckham.[3] It is important to realize that we are dealing here with two time scales.[16] The value $C_{s,f}$, which is reached within a few hours, corresponds to the end of an adsorption regime which is driven by the existence of free $AlOH_2^+$ sites. Once all sites are occupied, further adsorption needs ion-pair dissociation and reconformation of previously adsorbed polymers, a process which is comparatively slower.

Barford et al. inspired by the experiments of Klein and Luckham proposed a theory of polyelectrolyte adsorption in which they suppose sequential adsorption.[17] The first polymer that diffuses and sticks on the bare surface adopts a narrow concentration profile (flat configuration). It is very strongly bound, and a second polymer cannot displace it in any way, and so it binds less tightly. This picture is to some extent in the line of the mechanism we propose. Nevertheless, their theory is based on equilibrium conformations calculated via the self-consistent-field calculation for neutral polymers.[18] This is somewhat contradictory with the idea of tight binding, without displacement. Instead, we suppose that at a finite rate of injection no polymer is adsorbed in its equilibrium state.

Conclusion

The adsorption of hydrolyzed polyacrylamide onto an amphoteric surface was investigated as a function of pH. The isotherms determined in batch experiments exhibit at a pH below the isoelectric point a maximum with a negative slope at larger polymer concentration. This feature and the slow increase with time of the adsorption amount were interpreted assuming a slow conformational change of preadsorbed polymers, which proceeds through the release of ion pairing. A continuously stirred tank reactor was then used to monitor the kinetics of adsorption. Several important points could be reached in performing kinetically controlled adsorption runs: (i) The adsorption amount depends on the way the surface layer is built. This suggests irreversible behavior beyond the scope of equilibrium theories. (ii) The rate of adsorption is governed by the sign of the surface charge. Near the isoelectric point, self-induced surface charges lead to a remarkable cooperative effect in the kinetics of adsorption.

Acknowledgment. This work was supported by the Institut Français du Pétrole. We thank Dr. G. Chauveteau for discussions and the I.F.P. for financial support (A. C. Jean-Chronberg).

Appendix

Cooperativity in Polyelectrolyte Adsorption (Simplified Model). The diffuse polymer layer is replaced by a layer of thickness a, with a uniform smeared charge density ρ_p:

$$\rho_p = -\frac{NeC_p\alpha\tau}{aM} \tag{A1}$$

C_p is the concentration of polymer adsorbed per unit surface, e the elementary charge, M the mass of a monomer, α and τ the degree of ionization and hydrolysis, respectively, and N the Avogadro number. The electrostatic potential ψ in region I, containing the polymer layer, and region II, devoid of polymer, is given by the Poisson–Boltzmann equation:

$$\frac{d^2\psi}{dx^2} = -\frac{1}{\epsilon}\left(\rho_p + eC_s\left[\exp\left(-\frac{e\psi}{kT}\right) - \exp\left(\frac{e\psi}{kT}\right)\right]\right) \tag{A2}$$

C_s is the electrolyte concentration in the bulk and ϵ the permittivity. The boundary conditions at $x = a$ are

$$\psi_{I,x=a} = \psi_{II,x=a} \tag{A3}$$

$$\left.\frac{d\psi_I}{dx}\right|_{x=a} = \left.\frac{d\psi_{II}}{dx}\right|_{x=a} \tag{A4}$$

Equation A2 can be solved when the exponentials are linearized; i.e., in the approximation of Debye–Hückel, we find for region I

$$\psi = \frac{eb(\beta_1 - \beta_2)}{\epsilon\kappa}\exp(-\kappa x) - \frac{\rho_p}{\epsilon\kappa^2}(\exp[-\kappa(a-x)] + \exp[-\kappa(a+x)] - 2) \tag{A5}$$

b is the number of Al per unit surrace area, and $b\beta_1$ and $b\beta_2$ are respectively the number of $AlOH_2^+$ and AlO^- groups per unit surface area. The surface charge density is

$$\sigma = eb(\beta_1 - \beta_2) \tag{A6}$$

and κ is the Debye–Hückel screening length

$$\kappa^2 = \frac{2e^2C_s}{\epsilon kT} \tag{A7}$$

The charge densities β_1 and β_2 can be computed from the acid and base reaction of $(SiO)_2AlOH$

$$2.3\text{pH} + \ln\left[\frac{\beta_1}{1-(\beta_1+\beta_2)}\right] + \frac{e\psi_0}{kT} = 2.3\text{p}K_1^\circ \tag{A8}$$

ψ_0 is the surface potential. With $x = 0$ in eq A5 we obtain

$$2.3kT(\text{pH} - \text{p}K_1^\circ) + kT\ln\left[\frac{\beta_1}{1-(\beta_1+\beta_2)}\right] + \frac{e^2b}{\epsilon\kappa}(\beta_1 - \beta_2) = -\frac{e^2C_p\alpha\tau}{M\epsilon\kappa^2 a}[\exp(-\kappa a) - 1] \tag{A9}$$

Since $\exp(-\kappa a) - 1$ is a negative quantity, the right-hand side of eq A9 positive. Therefore, β_1, the density of $AlOH_2^+$, increases with C_p and β_2 decreases.

References and Notes

(1) Cohen Stuart, M. A.; Tamai, H. *Langmuir* **1988**, *4*, 1184.
(2) Cohen Stuart, M. A.; Tamai, H. *Macromolecules* **1988**, *21*, 1863.
(3) Klein, J.; Luckham, P. F. *Macromolecules* **1984**, *17*, 1041.
(4) Pefferkorn, E.; Carroy, A.; Varoqui, R. *J. Polym. Sci.* **1985**, *23*, 1997.
(5) Pefferkorn, E.; Jean-Chronberg, A. C.; Chauveteau, G.; Varoqui, R. *J. Colloid Interface Sci.*, in press.
(6) Truong Minh, N. Thesis, University Louis Pasteur, Strasbourg, France, 1984.
(7) Pefferkorn, E.; Carroy, A.; Varoqui, R. *Macromolecules* **1985**, *18*, 2253.
(8) Pefferkorn, E.; Haouam, A.; Varoqui, R. *Macromolecules* **1989**, *22*, 2677.
(9) Sears, G. W. *Anal. Chem.* **1956**, *28*, 1981.
(10) Varoqui, R.; Pefferkorn, E. *Makromol. Chem. Symp.* **1988**, *17*, 87.
(11) Stromberg, R. R.; Smith, L. E.; McCrackin, F. L. *Symp. Faraday Soc.* **1970**, *4*, 192.
(12) Kawaguchi, M.; Hayakawa, K.; Takahashi, A. *Polym. J. (Tokyo)* **1980**, *12*, 265.
(13) Joppien, G. R. *J. Physical Chem.* **1978**, *82*, 2210.
(14) Foissy, A.; El Attar, A.; Lamarche, J. M. *J. Colloid Interface Sci.* **1983**, *26*, 273.
(15) Varoqui, R.; Tran, Q. K.; Pefferkorn, E. *Macromolecules* **1979**, *12*, 831.
(16) Pefferkorn, E.; Jean-Chronberg, A. C.; Varoqui, R. *C. R. Acad. Sci. Paris, Ser. 2* **1989**, *308*, 1203.
(17) Barford, W.; Ball, R. C.; Nex, C. M. M. *J. Chem. Soc., Faraday Trans.* **1986**, *82*, 3233.
(18) de Gennes, P.-G. *Scaling Concepts in Polymer Physics*; Cornell University Press: Ithaca, NY, 1979; p 252.